Proceedings of the ASME 2024 43nd International Conference on Ocean, Offshore and Arctic Engineering
OMAE2024
June 9-14, 2024, Singapore EXPO, Singapore

OMAE2024-126186

PREDICTION OF GLOBAL WHIPPING RESPONSES ON A LARGE CRUISE SHIP UNDER UNKNOWN SEA STATES USING AN LSTM BASED ENCODER-DECODER MODEL

Ruixiang Liu
College of Shipbuilding Engineering,
Harbin Engineering University
Harbin, China

Hui Li
College of Shipbuilding Engineering,
Harbin Engineering University
Harbin, China

Muk Chen Ong
Department of Mechanical and Structural Engineering and Materials Science,
University of Stavanger
Stavanger, Norway

Jian Zou
College of Shipbuilding Engineering,
Harbin Engineering University
Harbin, China

ABSTRACT

Global whipping responses, characterized by high-frequency vibration components on the hull girder, are typically induced by stern and bow slamming loads. These responses contribute to an increase in vertical bending moments, making their accurate prediction crucial for ship safety. This study introduces a novel approach to predict these responses using a Long Short-Term Memory (LSTM) based encoder-decoder model. The model is trained on a comprehensive dataset, which includes motion data and vertical bending moment history of a large cruise ship under various sea states. This dataset is established via numerical simulation, ensuring a wide range of scenarios for the model to learn from. The efficacy of the LSTM encoder-decoder model in capturing global whipping responses is initially verified under a single sea state case. This step confirms the model's ability to accurately predict vertical bending moments under known conditions. Subsequently, the model's performance under unknown sea states is examined. Given that the distribution of training data significantly influences the model's performance under unknown sea states, a data mixing strategy is employed during the training process in this scenario. The results indicate that the LSTM encoder-decoder model effectively captures whipping responses. Furthermore, the data mixing strategy significantly improves prediction accuracy under unknown sea states, demonstrating the potential of this approach in enhancing ship safety.

Keywords: Multivariate time series forecasting; whipping response; machine learning

1. INTRODUCTION

Whipping responses are significant threats to vessels, since these high-frequency vibrations on the hull girder contribute to an increase in Vertical Bending Moments (VBM)[1–3]. These global whipping responses are typically induced by a strong pulse excitation, such as slamming, and represent a form of fluid-structure interaction. Traditionally, simulation of these responses necessitates a numerical method comprising three components: a fluid solver for addressing the seakeeping problem, a structural solver for handling flexible vibrations, and a slamming solver to deal with slamming loads. Based on this framework, Kim et al. proposed a numerical analysis method utilizing a 3-D Rankine panel method, 1-D/3-D finite element methods and a 2-D generalized Wagner method to investigate whipping of a containership in regular waves[4]. Jiao et al. developed a time-domain hydro-elasticity method with potential flow theory to investigate the whipping loads in harsh irregular seaways[5]. Lu et al. adopted the modified Logvinovich method to investigate the hydro-elastic responses of a 21,000 TEU container ship, and the asymmetric slamming is taken into account[6]. Lakshmynarayanana and Temarel coupled the Computational Fluid Dynamics (CFD) tools with Finite Element Analysis (FEA) methods to develop a two-way partitioned way for calculating the whipping and springing responses[7]. Jiao et al. also used a two-way fluid-structure interaction of CFD-FEA coupling method to predict the global ship motions, wave loads and springing and whipping responses of the S175 ship[8].

In past few years, artificial intelligence technology has gradually become a research hotspot, with related applications emerging increasingly. There is limited research on using artificial neural network (ANN) methods to predict the wave loads on vessels. Xu firstly applied ANN in the area of linear wave loads estimation[9,10]. Moreira and Soares also established a time-domain technique based on ANN for estimating linear wave-induced ship hull bending moment and shear force from ship motions[11]. Liu et al. proposed a method based on Long Short-Term Memory (LSTM) model to

investigate the prediction of global whipping responses for the first time[12].

In contrast to traditional numerical methods, ANN possesses the ability to rapidly solve computationally intensive problems as a soft computing approach. This renders it a promising tool for wave loads prediction, where swift prediction methods can enhance vessel operation and safety, and support decision-making processes for autonomous ships. However, existing research primarily focuses on predictions under known sea states. Given that sea conditions encountered by vessels are diverse and unpredictable, the ability of ANN to generalize and predict wave loads under unknown sea states is crucial for practical application. In sight of this, an LSTM based encoder-decoder model is proposed in this study. The model's ability to capture and predict the global whipping responses is validated under a known sea state. Moreover, the generalization of the model under unknown sea states is evaluated, and a mixed data training strategy is proved to effectively enhance the model's generalization.

2. METHODOLOGY AND NUMERICAL SETUP

2.1. LSTM based encoder-decoder model

A typical encoder-decoder model contains two parts, as illustrated in FIGURE 1: the encoder part which distills the important information encapsulated in the inputs and encodes them in a state vector; and the decoder one which leverages the state vector to generate predictions.[13] The whole model is designed to model a conditional probability as shown in equation (1) :

$$P(y_{T_{in}},\cdots,y_{T_{out}} \mid x_1,\cdots,x_{T_{in}}) \tag{1}$$

where x_t and y_t denotes the input at t instant, respectively. T_{in} is the input sequence length, and $T_{out}-T_{in}$ refers to the prediction horizon.

In the present study, $\{x_t\}_{t=1}^{T_{in}}$ represents a multivariate input sequence which contains the ship motion and wave elevation data in the past T_{in} time period. While, $\{y_t\}_{t=T_{in}}^{T_{out}}$ represents the predicted vertical bending moments (VBM) from T_{in} to T_{out}. At the encoding stage, through LSTM units, x_t is sequentially encoded into h_t and c_t , which denotes the hidden state and cell state of the encoder LSTM. This process can be explained mathematically in equations (2) - (7):

$$f_t = \sigma(W_{hf}h_{t-1} + W_{xf}x_t + b_f) \tag{2}$$
$$i_t = \sigma(W_{hi}h_{t-1} + W_{xi}x_t + b_i) \tag{3}$$
$$\tilde{C}_t = \tanh(W_{hc}h_{t-1} + W_{xc}x_t + b_c) \tag{4}$$
$$c_t = f_t \cdot c_{t-1} + i_t \cdot \tilde{C}_t \tag{5}$$
$$o_t = \sigma(W_{ho}h_{t-1} + W_{xo}x_t + b_o) \tag{6}$$
$$h_t = o_t \cdot \tanh(c_t) \tag{7}$$

where, W_{ij} represents the weight matrix between vector i and j ; b denotes the bias; tanh(*) and σ(*) means the hyperbolic tangent function and the sigmoid function, respectively; f_t , i_t and o_t are three unique structures of the LSTM unit, respectively referred as to the forget gate, input gate and output gate. The detailed structure of the LSTM unit is depicted in FIGURE 2.

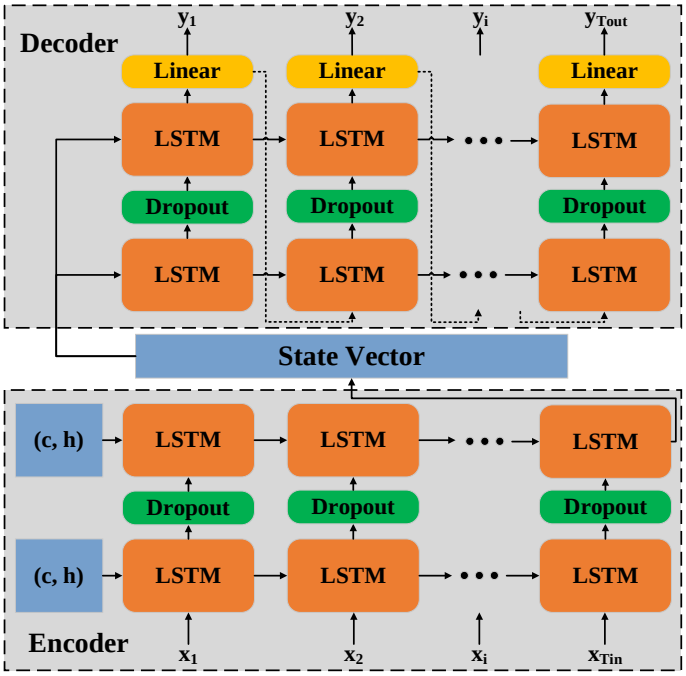

FIGURE 1 THE ARCHITECTURE OF THE LSTM BASED ENCODER-DECODER MODEL

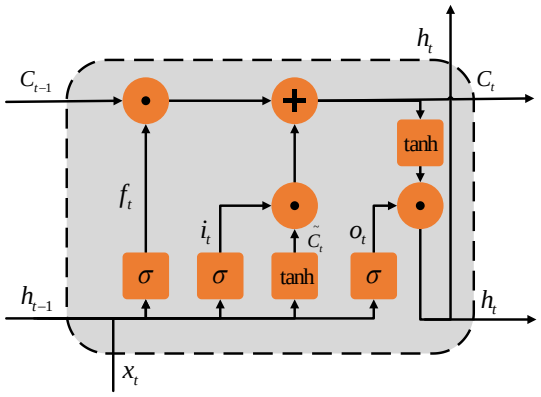

FIGURE 2 THE SCHEMA OF A TYPICAL STRUCTURE OF AN LSTM UNIT

After the encoding stage, the terminal state vector $(h_{T_{in}}, c_{T_{in}})$ is used in the decoding stage as the representation of the input sequence. At the decoder stage, the output sequence $\{y_t\}_{t=T_{in}}^{T_{out}}$ is predicted recursively as shown in equation (8):

$$y_t = g(LSTM(y_{t-1}, h_{t-1}, c_{t-1}; (h_{T_{in}}, c_{T_{in}}))) \quad (8)$$

where $g(*)$ refers to a fully connected layer applied after the LSTM layer, and $LSTM(*)$ means the function of LSTM units, as shown in equations (2) - (7). Note that the final state vector of the encoding stage $(h_{T_{in}}, c_{T_{in}})$ has an implicit impact on the prediction of y_t in the decoding stage as shown in equation (8), as this terminal state is used as the initial state of LSTM decoder.

2.2. Dataset

In the present study, the VBM time history of a large cruise is predicted using the LSTM encoder-decoder model. The principal dimensions of the cruise are listed in TABLE 1.

TABLE 1 PRINCIPAL DIMENSIONS OF THE CRUISE

Properties	Value
Length (m)	322.1
Length between perpendiculars (m)	294.6
Beam (m)	37.2
Depth (m)	29.65
Draft (m)	8.6
Displacement (ton)	71,112
Vertical center of gravity (m)	17.96
Longitudinal center of gravity (m)	151.9
Wet natural frequency of the first order vertical bending vibration (Hz)	1.065

To ensure the sufficiency of the dataset, the global responses of the cruise are numerically simulated via a time-domain hydro-elastic numerical code[14], which integrates a beam model, the 3-D Rankine panel model and the 2-D modified Logvinovich model to deal with the hydro-elastic responses. FIGURE 3 shows the panel mesh of the cruise used in the numerical simulation. The VBM at the midship, along with the heave and pitch motion data, the vertical accelerations at the stern, bow and midship, as well as the wave elevations at stern and bow are collected through the numerical simulations. These data are used to set up a comprehensive dataset under five different irregular wave conditions, as listed in TABLE 2. Within these time series data, the VBM time sequences are designated as the target output, whereas the remaining motion and wave data serve as the input sequences.

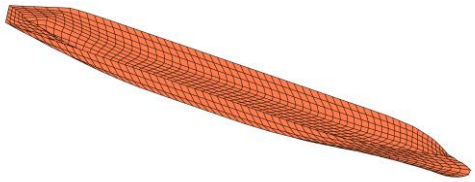

FIGURE 3 THE PANEL MESH OF THE CRUISE

Considering the disparate dimensions and magnitudes of the input and output data. It becomes imperative to normalize the original dataset to mitigate the risk of network calculation errors caused by the differences in the order of magnitude. The standard normalization method is employed in this study, as expressed in equation (9):

$$x_{norm} = \frac{x_{original} - \mu_{train}}{\sigma_{train}} \quad (9)$$

where, $x_{original}$, μ_{train}, σ_{train} represent the original data, the mean value of original train data and the standard deviation of original train data, respectively. x_{norm} means the normalized data. This normalization process must be carried out on the whole dataset prior to its importation into the network. Once the calculation of the network has been done, the output data calculated by the network must be denormalized to generate the actual results with the proper dimension, as shown in equation (10):

$$x_{actual} = x_{norm} \cdot \sigma_{train} + \mu_{train} \quad (10)$$

TABLE 2 SIMULATION CONDITIONS

Case	Heading	Spectrum	Spectral peak period (s)	Significant wave height (m)	Speed (kn)	Simulation duration (s)	Time step (s)
Sea state 1	Head sea	ITTC two-parameter spectrum	11.5	7.5	0	3600	0.1
Sea state 2				9.5			
Sea state 3				11.5			
Sea state 4				13.5			
Sea state 5				15.5			

2.3. Evaluation index

Four statistical indices are adopted in this study to assess the performance of the model, as expressed by equations (11)-(14):

$$NMAE = \frac{\frac{1}{n}\sum_{i=1}^{n}|y_i^{true} - y_i^{pred}|}{y_{std}^{true}} \tag{11}$$

$$NRMSE = \frac{\sqrt{\frac{1}{n}\sum_{i=1}^{n}(y_i^{true} - y_i^{pred})^2}}{y_{std}^{true}} \tag{12}$$

$$CC = \frac{\sum_{i=1}^{n}(y_i^{true} - \bar{y}^{true})(y_i^{pred} - \bar{y}^{pred})}{\sqrt{\sum_{i=1}^{n}(y_i^{true} - \bar{y}^{true})^2 \sum_{i=1}^{n}(y_i^{pred} - \bar{y}^{pred})^2}} \tag{13}$$

$$R^2 = 1 - \frac{\sum_{i=1}^{n}(y_i^{true} - y_i^{pred})^2}{\sum_{i=1}^{n}(y_i^{true} - \bar{y}^{true})^2} \tag{14}$$

where NMAE, NRMSE, CC and R^2 refer to the four evaluation indices: non-dimensional mean absolute error, non-dimensional root mean square error, correlation coefficient and coefficient of determination, respectively; n means the data length; y_i represents the value at i instant; the subscript std suggests the standard deviation value; the overline sign denotes the average value. Generally, as the predicted values converge towards the target values, the indices CC and R^2 tend towards 1, while the values of NMAE and NRMSE approach 0.

2.4. Determination of the optimal model structure

The performance of the neural networks is concerned with the selection of hyperparameters. In order to determine the optimal model structure, a comprehensive grid search of the appropriate hyperparameters is performed on the data under sea state 1. The final determined hyperparameters are listed in TABLE 3

TABLE 3 HYPERPARAMETER TUNING VALUES AND RESULTS

Parameter	Search domain	Final value
Encoder LSTM layers	[1, 5]	2
Decoder LSTM layers	[1, 5]	2
Hidden units	{8, 16, 32, 64, 128}	64
Batch size	{16, 32, 64, 128, 256}	64
Learning rate	{1e^{-2}, 1e^{-3}, 1e^{-4}}	1e^{-3}
Dropout rate	[0, 0.1, 0.2, 0.3]	0.2

3. RESULTS AND DISCUSSION

In this section, the performance of the established encoder-decoder model in predicting VBM is investigated. Initially, prediction under a single state is conducted to verify the capability of the model to capture the relationship between the motion data and global whipping responses. Subsequently, a data mixing strategy is employed to augment the generalization ability of the model, and the prediction performance under unknown sea states of the model is evaluated.

3.1. Prediction under known sea state

The prediction performance of the model is verified under sea state 3. The original dataset, exclusively collected under this specific sea state, has been independently pre-split into a training set and a test set at a ratio of 4:1 prior to the beginning of the training process. The model firstly undergoes the training phase on the training set over the course of 100 epochs. Subsequently, the well-trained model is tested on the test set. The prediction horizon is set as 3 seconds. It is noteworthy that despite both the training set and the test set being collected under an identical sea state, the test set is never exposed to the model during the training stage. This ensures validity of the testing process.

TABLE 4 STATISTICAL INDICES OF PREDICTION RESULTS UNDER KNOWN SEA STATE

Case	NMAE	NRMSE	CC	R^2
Sea state 3	0.146	0.238	0.958	0.912

TABLE 4 lists the statistical indices of the prediction results under sea state 3. The value of NMAE and NRMSE is 0.146 and 0.238, respectively. Furthermore, both the CC and R^2 exceed 0.9. All indices demonstrate a good performance in predicting the VBM time series.

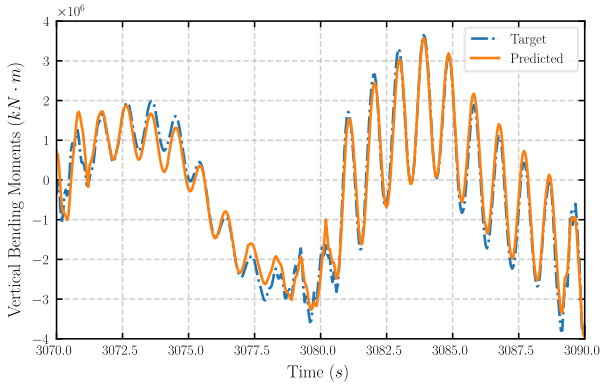

FIGURE 4 THE COMPARISON BETWEEN THE TIME SERIES OF THE PREDICTED VBM AND THE TARGET ONE

FIGURE 4 shows a comparison between the predicted VBM and the target time series. It is evident that the model accurately predicts not only the overall trend of the VBM time series, but also its details. FIGURE 5 illustrates a comparative analysis between the spectrum of the predicted VBM and the target one. There are two primary peaks observed: the lower frequency one is located at around 0.087 Hz and the higher frequency one is situated approximately at 1.065 Hz. These two peaks correspond respectively to the linear wave-frequency response (with a spectral peak frequency of 0.087 Hz) and the first order vertical bending vibration (with a wet natural frequency in still water of

1.065 Hz). The convergence of the predicted spectrum with the target one indicates that the model effectively captures both the wave-frequency vibrations and the first-order whipping responses.

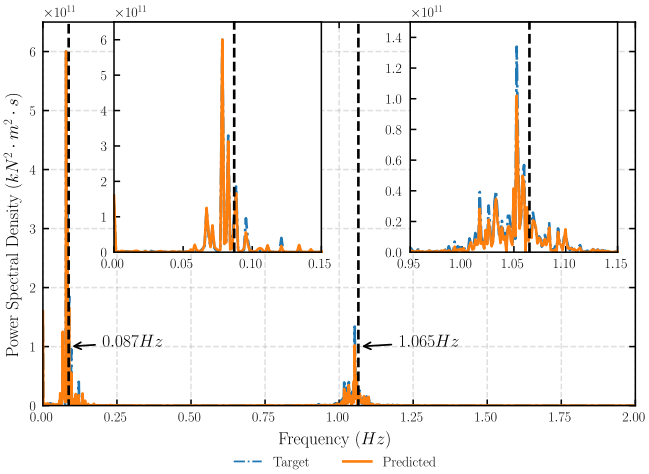

FIGURE 5 THE COMPARISON BETWEEN THE SPECTRUM OF THE PREDICTED VBM AND THE TARGET ONE

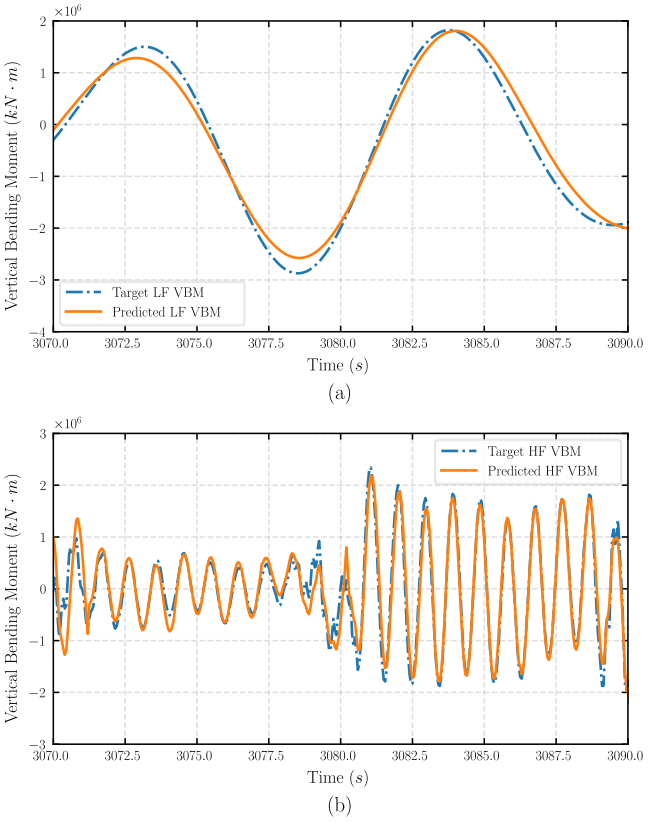

FIGURE 6 (A) THE COMPARISON BETWEEN THE PREDICTED LOW-FREQUENCY VBM AND THE TARGET ONE; (B) THE COMPARISON BETWEEN THE PREDICTED HIGH-FREQUENCY VBM AND THE TARGET ONE

FIGURE 6 provides more intuitive evidences. In this figure, the time series of both the predicted VBM and the target one are divided into low-frequency and high-frequency components, using a cutoff frequency that is twice the spectral peak frequency. The corresponding statistical indices for the low-frequency and the high-frequency components are listed in TABLE 5. It can be observed that the model exhibits commendable performance in predicting both the low-frequency responses and the high-frequency components under a known sea state.

TABLE 5 STATISTICAL INDICES FOR DIFFERENT COMPONENTS OF VBM

Component	NMAE	NRMSE	CC	R^2
Low-frequency	0.124	0.159	0.977	0.964
High-frequency	0.161	0.323	0.947	0.876

3.2. Prediction under unknown sea state

Given the transient nature of the sea conditions encountered by vessels during navigation, the generalization ability of the model to predict VBM under unknown sea states is of vital importance. In this section, five cases are established to investigate the prediction of VBM under the unknown sea state. As shown in TABLE 6, all models, irrespective of the case, are tested under a same unknown sea state, which is sea state 3. For cases C1 to C4, the training set is confined to a single sea state, whereas case C5 adopts a strategy of training with mixed sea state data. To avoid the potential impact of variations in the size of the training set adopted by different training strategies on prediction accuracy, the size of the training and test sets used in all cases under the unknown sea state is maintained to be consistent with that used in the known sea state case. This ensures a standardized comparison.

TABLE 6 THE SETUP OF THE CASES FOR PREDICTION UNDER UNKNOWN SEA STATES

Case	Training set	Test set
C1	Sea state 1	Sea state 3
C2	Sea state 2	
C3	Sea state 4	
C4	Sea state 5	
C5	Mixed sea states (Sea state 1, 2, 4 and 5)	

FIGURE 7 illustrates the time series of the predicted VBM for the five cases under consideration. Corresponding statistics are detailed in TABLE 7. As anticipated, the model's performance in predicting VBM under an unknown sea state is inferior to that under a known sea state. However, the model's performance significantly improves when employing a mixed data strategy (Case C5), compared to the model trained with data from a single sea state (Cases C1 to C4). In fact, when evaluated against the benchmark of R^2, the performance of case C5 is

only marginally inferior by 2.30% to the performance of prediction made under a known sea state.

TABLE 7 STATISTICAL INDICES FOR PREDICTION UNDER SEA STATE 3

Case	NMAE	NRMSE	CC	R^2
C1	0.299	0.476	0.893	0.592
C2	0.273	0.438	0.900	0.743
C3	0.245	0.398	0.918	0.826
C4	0.263	0.447	0.899	0.796
C5	0.203	0.330	0.946	0.891

FIGURE 8 presents the correlation between the target and predicted results under cases C2, C3, and C5. Each of these three cases represents a unique training strategy: C2 utilizes data from a lower single sea state for training, C3 is trained on data under a higher single sea state, and C5 employs a mixed data training strategy. In FIGURE 8, the solid line stands for the linear fitting of the data points using the least squared method, and the dashed line refers to the bisector. The convergence between the predicted VBM and the target results increases as the linear fitting line approaches the bisector. The slope of the linear fitting line for case C5 (FIGURE 8 (c)) is 0.944, indicating a strong agreement with the bisector. In contrast, the slope for case C2 is 0.777, significantly less than 1.0, and the spread of the data is smaller than the other two. Conversely, the slope for case C3 is 1.105, exceeding 1.0 by 0.105, and exhibits the most pronounced data spread among these three cases. The difference in the slopes of the fitting lines across these three cases can be attributed to the varying training strategies: Specifically, the model trained under case C2 tends to underpredict the VBM, as the sea state used for training is lower than that used for testing, resulting in a smaller slope of the fitting line. For case C3, the higher training sea state leads to overpredicted results. However, in case C5, the adoption of a mixed data training strategy allows the model to be trained under various sea states, enhancing the model's generalizability to unseen sea states.

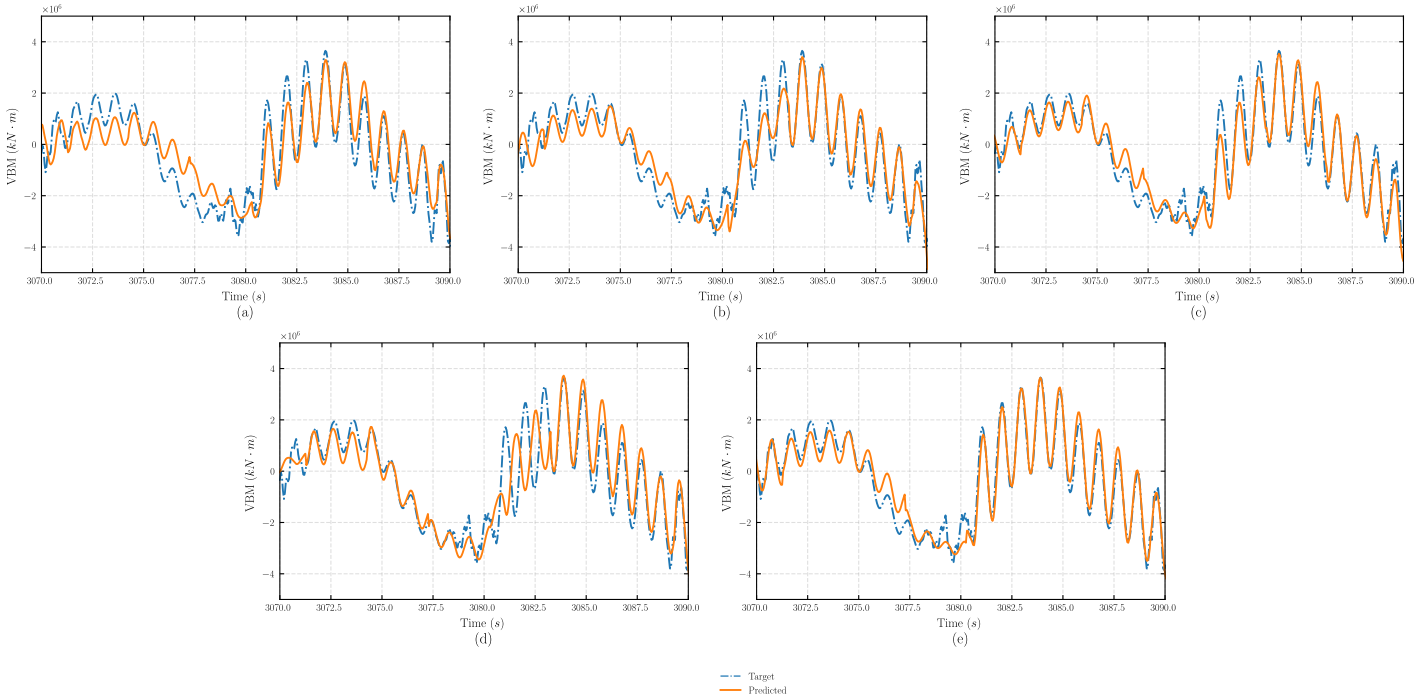

FIGURE 7 THE COMPARISON OF THE PREDICTED VBM UNDER SEA STATE 3 FOR DIFFERENT TRAINING STRATEGIES: (A) CASE C1; (B) CASE C2; (C) CASE C3; (D) CASE C4; (E) CASE C5.

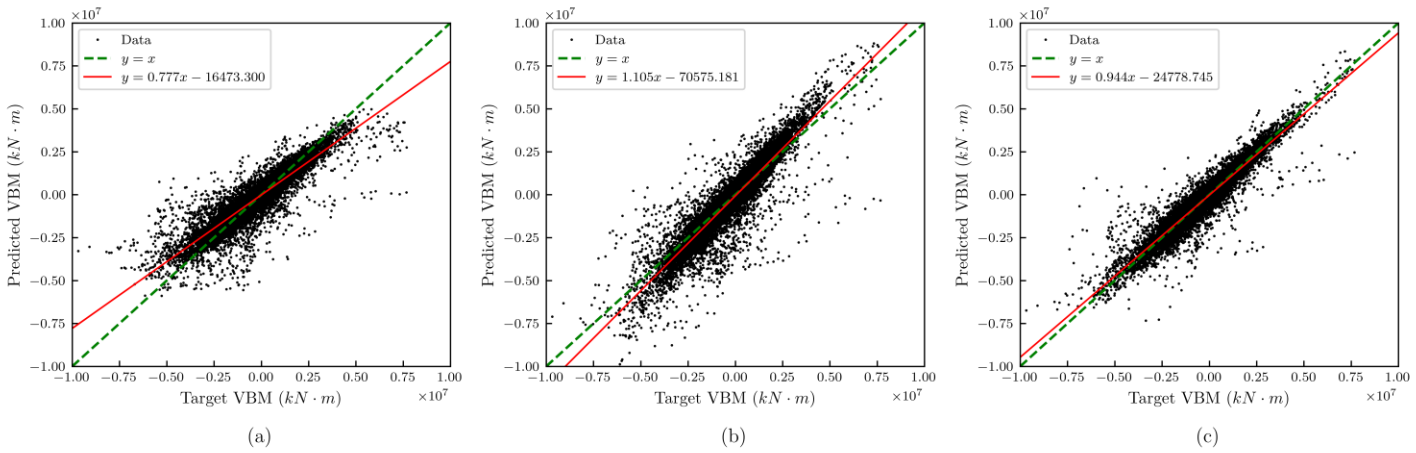

FIGURE 8 THE COMPARISON BETWEEN THE TARGET AND PREDICTED RESULTS UNDER: (A) CASE C2; (B) CASE C3; (C) CASE C5.

4. CONCLUSION

In this study, an encoder-decoder model based on LSTM is developed to predict the global whipping responses of a large cruise ship. The original dataset, comprising motion data, wave elevation data, and corresponding VBM under five distinct sea states, is numerically simulated using a time-domain hydro-elastic numerical code. The LSTM based encoder-decoder model is subsequently trained on various cases to investigate the prediction of VBM under known and unknown sea states. It is found that the established model is capable of accurately capturing the whipping responses and predicting the time series of VBM. In the case study focusing on the prediction under an unknown sea state, the mixed data training strategy is proved to be effective. This strategy enhances the model's ability to generalize and predict the VBM under unfamiliar sea states, thereby demonstrating its potential for practical applications in maritime engineering.

ACKNOWLEDGEMENTS

This research was funded by National Natural Science Foundation of China (No. 52071110)

REFERENCES

[1] Drummen, I., Wu, M., and Moan, T., 2009, "Experimental and Numerical Study of Containership Responses in Severe Head Seas," Marine Structures, **22**(2), pp. 172–193.

[2] Bahamas Maritime Authority, 2015, *Report of the Investigation into the Sinking of the "MOL Comfort" in the Indian Ocean*.

[3] Marine Accident Investigation Branch, 2008, *Investigation Report MSC Napoli*, Report No 9/2008, UK.

[4] Kim, J.-H., Kim, Y., Yuck, R.-H., and Lee, D.-Y., 2015, "Comparison of Slamming and Whipping Loads by Fully Coupled Hydroelastic Analysis and Experimental Measurement," Journal of Fluids and Structures, **52**, pp. 145–165.

[5] Jiao, J., Yu, H., Chen, C., and Ren, H., 2019, "Time-Domain Numerical and Segmented Model Experimental Study on Ship Hydroelastic Responses and Whipping Loads in Harsh Irregular Seaways," Ocean Engineering, **185**, pp. 59–81.

[6] Lu, L., Ren, H., Li, H., Zou, J., Chen, S., and Liu, R., 2023, "Numerical Method for Whipping Response of Ultra Large Container Ships under Asymmetric Slamming in Regular Waves," Ocean Engineering, **287**, p. 115830.

[7] Lakshmynarayanana, P. A., and Temarel, P., 2020, "Application of a Two-Way Partitioned Method for Predicting the Wave-Induced Loads of a Flexible Containership," Applied Ocean Research, **96**, p. 102052.

[8] Jiao, J., Huang, S., and Guedes Soares, C., 2021, "Viscous Fluid–Flexible Structure Interaction Analysis on Ship Springing and Whipping Responses in Regular Waves," Journal of Fluids and Structures, **106**, p. 103354.

[9] Xu, J., 2000, "Estimation of Wave-Induced Ship Hull Bending Moment from Ship Motion Measurements," Ph.D. Thesis, Faculty of Engineering and Applied Science Memorial University of Newfoundland.

[10] Xu, J., and Haddara, M. R., 2001, "Estimation of Wave-Induced Ship Hull Bending Moment from Ship Motion Measurements," Marine Structures, **14**(6), pp. 593–610.

[11] Moreira, L., and Soares, C. G., 2020, "20.Neural Network Model for Estimation of Hull Bending Moment and Shear Force of Ships in Waves," Ocean Engineering, **206**, p. 107347.

[12] Liu, R., Li, H., Zou, J., and Ong, M. C., 2023, "Reconstruction and Prediction of Global Whipping Responses on a Large Cruise Ship Based on LSTM Neural Networks," Ocean Engineering, **285**, p. 115393.

[13] Cho, K., van Merrienboer, B., Gulcehre, C., Bahdanau, D., Bougares, F., Schwenk, H., and Bengio, Y., 2014, "Learning Phrase Representations Using RNN Encoder-Decoder for Statistical Machine Translation."

[14] Li, H., Zou, J., Peng, Y., Zhou, X., Lu, L., and Sun, S., 2024, "Numerical Study of Slamming and Whipping Loads in Moderate and Large Regular Waves for Different Forward Speeds," Marine Structures, **94**, p. 103563.